

An open source GPS multipath simulator in Matlab/Octave

Felipe G. Nievinski · Kristine M. Larson

Received: 30 September 2013 / Accepted: 17 February 2014
© Springer-Verlag Berlin Heidelberg 2014

Abstract Multipath is detrimental for both GPS positioning and timing applications. However, the benefits of GPS multipath for reflectometry have become increasingly clear for monitoring soil moisture, snow depth, and vegetation growth. In positioning applications, a simulator can support multipath mitigation efforts in terms of, e.g., site selection, antenna design, receiver performance assessment, and in relating different observations to a common parameterization. For reflectometry, in order to convert observed multipath parameters into useable environmental products, it is important to be able to explicitly link the GPS observables to known characteristics of the GPS receiver/antenna and the reflecting environment. Existing GPS multipath software simulators are generally not readily available for the general scientific community to use and/or modify. Here, a simulator has been implemented

in Matlab/Octave and is made available as open source code. It can produce signal-to-noise ratio, carrier phase, and code pseudorange observables, based on L1 and L2 carrier frequencies and C/A, P(Y), and L2C modulations. It couples different surface and antenna types with due consideration for polarization and coherence. In addition to offering predefined material types (water, concrete, soil, etc.), it allows certain dimensional properties to be varied, such as soil moisture and snow density.

Keywords GPS · GNSS · Multipath · Reflectometry · Coherent · Simulator · Simulation

Introduction

Nievinski and Larson (2014a) presented a forward multipath model for near-surface reflectometry and positioning applications. While that research paper formulated and illustrated the model, the present short companion paper focuses on the simulation software. It has been implemented in Matlab/Octave and is made available as open source code. It can produce signal-to-noise ratio (SNR), carrier phase, and code pseudorange observables, based on L1 and L2 carrier frequencies and C/A, P(Y), and L2C modulations. It couples different surface and antenna types with due consideration for polarization and coherence. In addition to offering predefined material types (water, concrete, soil, etc.), it allows certain dimensional properties to be varied, such as soil moisture and snow density. The source code is available at the GPS Toolbox Web site (<http://www.ngs.noaa.gov/gps-toolbox>); it includes both the simulator software library as well as driver scripts to generate all figures in both papers.

The GPS Tool Box is a column dedicated to highlighting algorithms and source code utilized by GPS engineers and scientists. If you have an interesting program or software package you would like to share with our readers, please pass it along; e-mail it to us at gpstoolbox@ngs.noaa.gov. To comment on any of the source code discussed here, or to download source code, visit our website at <http://www.ngs.noaa.gov/gps-toolbox>. This column is edited by Stephen Hilla, National Geodetic Survey, NOAA, Silver Spring, Maryland, and Mike Craymer, Geodetic Survey Division, Natural Resources Canada, Ottawa, Ontario, Canada.

F. G. Nievinski (✉)
Departamento de Cartografia, Faculdade de Ciências e
Tecnologia, Universidade Estadual Paulista Júlio de Mesquita
Filho, Presidente Prudente, SP, Brazil
e-mail: fgnievinski@gmail.com

K. M. Larson
Department of Aerospace Engineering Sciences,
University of Colorado, Boulder, CO, USA

Background

Although simulations are rarely sufficiently accurate to be used as measurement corrections for multipath mitigation in GPS positioning applications, their error envelopes are often useful as bounds on the expected uncertainty, for use in performance integrity in navigation augmentation (Cox et al. 2000; Macabiau et al. 1999) and stochastic weighting in geodesy (Luo et al. 2008). Furthermore, by offering repeatable conditions, a simulator can serve as a neutral criterion in the comparison of competing architectures (Irsigler et al. 2005) and in the impact assessment of positioning solutions (King and Watson 2010). Finally, in principle, measurements could be used to estimate improved values for the underlying parameters driving the simulation, leading to potentially more accurate corrections for multipath errors (Bilich et al. 2008). Multipath simulators have also been used for the assessment of proposed site installations (Weiss et al. 2007).

In parallel to efforts to mitigate multipath by the positioning community, the reflectometry community has developed ways to exploit GPS reflections (GPS-R) for remote sensing of the environment. We concentrate on the single-antenna single-replica GPS-R mode, which we call GPS multipath reflectometry (GPS-MR). A multipath simulator supports GPS-MR in allowing the explicit linking of GPS observables to the equipment and environment characteristics. More specifically, simulators have been used in evaluating the theoretical performance of retrieval algorithms (Chew et al. 2013), the design of new instruments, site selection, and in quantifying the observation/parameter sensitivities for data inversion (Nievinski and Larson 2014b).

Other simulators

We identify three main types of GPS multipath simulations in the literature. Tracking simulators focus on the measurement/replica signal matching, often adopting arbitrary values for the reflection power, delay, phase, and Doppler. Geometrical simulators calculate the reflection delay based on a given surface geometry, receiver position, and satellite direction, but the reflection power often remains empirically defined. Polarimetric simulators account for the polarization matching between surface and antenna responses, yielding physically based complex reflection coefficients.

Table 1 summarizes and cites these contributions. Abbreviations are in the format “XYZ,” which consists of first-author single-character surname initial followed by two-digit publication year and an optional disambiguation suffix; e.g., N14a stands for Nievinski and Nievinski and Larson (2014a). When more than one related article is

Table 1 Classification of GPS multipath simulators reported in the literature

<i>Observable</i>	
Pseudorange	E89, R92, V92, A94, L96, B96, E96, B97, B98, M98, A99, M98, C00, R01, B01, B02, K04, E05, F05, I05, K06, R06, W07, G08, L08, C09, S09, Z09, C10, I10, N14a
Carrier phase	G88, R92, A94, E95, G95, L96, B96, B97, M98, A99, M98, B01, R01, B01, B03, F06, K06, L07, B08, K10, B11, L11, O11, S13, B13, N14a
SNR	E89, R92, A94, B98, H98, K98, A99, A00, B01, R01, T01, B01, B08, J08, C09, Z10, B11, R11, M12, S13, B13, N14a
Waveform	T01, S08, S09, C12
<i>Geometry</i>	
Horizontal	G88, E89, R92, A94, E95, G95, B98, K98, A99, M98, A00, B01, K04, F05, L07, B08, J08, L08, Z09, K10, Z10, L11, O11, R11, C12, M12, S13, N14a
Tilted	R01
Plates	E89, E96?, B01, B03, F05, L07, C09
Facets	E89, L96, M98, B01, K04, E05, F06, R06, W07, C09, C10, I10
Irregular	R11
Undulated	–
Spherical	B01, T01, B11
Current	E89, A94, H98, G08, S08, C09, C10, I10
<i>Material</i>	
PEC	G95, L96, B98, M98, B01, W07, G08, S08, L11
Dielectric	E89, R92, E96, H98, K98, A99, M98, A00, T01, K04, E05, F05, F06, R06, L07, J08, C09, C10, I10, K10, Z10, R11, C12, M2, B13, S13, N14a
<i>Antenna</i>	
Isotropic	R92, H98, K98, A99, M98, A00, T01, E05, F05, S08, F06, J08, L08, L11, R11, C12, M12
Far-field pattern	E89, G95, L96, E96, B98, M98, B01, K04, R06, L07, W07, L08, C09, C10, I10, K10, Z10, B13, S13, 14a
Coupled	G08
Antenna/material— <i>empirical</i> : G88, E95, B01, R01, B03, B08, Z09, B11, O11	
Antenna/material/geometry— <i>arbitrary</i> : V92, B96, B97, B98, C00, I05, K06	
<i>Code modulation</i>	
None	G88, E95, G95, K98, A00, B01, B03, E05, F06, B08, J08, L08, S08?, K10, Z10, L11, O11, R11, C12, M12, B13, N14a
Auto-correlation	E89, R92, V92, B96, E96, L96, K06, B97, B98, H98?, M98, A99, R01, T01, B01, K04, F05, I05, K06, R06, L07, W07, C09, C10, I10, B11, S13, N14a
Transfer function	S08, G08, C09
SDR	M98, K06, S09, Z09
Hardware	C00, K06, Z09
<i>Extra</i>	
Troposphere	A00, B01, T01, B11
Roughness	E89, K10, R11, N14a
Layering	J08, Z10, R11, C12
Statistical	V92, B96, B97, B98, K06, S08, S09, C10, B13
Doppler	E89, V92, A94, E96, B98, M98, B01, K06, C09, S08, S09, Z09, C10, B11, L13

available from the same author group, we list a single representative one, normally the latest or most comprehensive one. We have not included articles dealing primarily with measurement instead of simulation. We have excluded GPS-R simulators developed primarily for incoherent targets, even though they could in principle be modified for GPS-MR. We have also excluded coherent-target dual-replica GPS-R modes (either single- or dual-antenna), in which code matching is done in a master/slave channel configuration, i.e., separately for each direct and reflected signals (instead of a single matching against the composite direct-plus-reflection signal as in GPS-MR); likewise, replica-free direct-against-reflection GPS-R has been excluded. We did include GPS-MR employing correlation versus delay waveforms as observable, beyond just SNR, carrier phase, and pseudorange at peak correlation. We excluded studies of multipath properties that are not commonly or directly measured by a GPS receiver, such as line-of-sight visibility, interferometric Doppler or fading rates, and interferometric power distribution, etc. In terms of scattering source, we excluded atmospheric multipath (neutral or ionized layers and ducts) as well as electronic components (loading mismatch) and kept in the scope antenna installation (satellite body or ground monument) in addition to the built environment, not only natural surfaces (land, water, vegetation, etc.). As for the receiving platform altitude, we considered from near-surface (few-meter tall) to elevated (towers, cliffs) all the way up to low-Earth orbit.

Each type of simulator admits subtypes. For example, tracking simulators can neglect the code modulation; account for the code autocorrelation function, implementing a time-domain discriminator function (valid for well-defined discrete rays); utilize a spectral-domain transfer function (more appropriate for ill-defined diffuse scattering); sample the digital intermediate-frequency signal, IF (to be input to a software-defined receiver, SDR); generate the analog radio frequency signal, RF (to be hardware-fed directly to a conventional receiver, bypassing the antenna); or synthesize the wave field (which then excites an actual antenna).

Geometrical simulators can support different surface shapes. Horizontal surfaces are the simplest to model. Tilted surfaces offer more degrees of freedom to represent different orientations, though they are still infinite and planar. Finite plates offer great flexibility in modeling complex surfaces, such as those found in the built environment; in this case, the individual reflections are determined via ray tracing, based on hit-or-miss conditions for specular reflection. A faceted model is more rigorous, in that diffraction rays are accounted for in addition to reflected ones. An irregular model extends the horizontal model piecewise, allowing the calculation of propagation

delays considering horizontally varying surface height. An undulated model accounts additionally for changes in reflection phase and power dependent on the surface tangent and curvature, with effects such as cross-polarization, ray focusing and spreading, caustics, etc.; an undulated model may account for multiple distinct yet simultaneous reflections. Finally, a more specialized surface geometry is that of a spherical Earth, necessary for reflectometry from high-altitude platforms.

A departure from such ray-based methods are, e.g., parabolic equation and physical optics. These current-based methods replace individual rays in favor of a continuous charge distribution which is integrated throughout the surface—instead of traced at reflection and diffraction points—whereby every element produces a scattering field in all directions, albeit with varying weights based on its size and orientation.

Often a total polarization reversal upon reflection is assumed for simplicity, although this is strictly valid only for a perfectly electrically conducting surface—as if reflections could be suppressed by ensuring that the antenna will respond to RHCP only. A polarimetric simulator supports dielectric materials as well, for which the actual reflection polarization ellipticity can be calculated from first principles. The far-field antenna radiation patterns can then be matched with each co- and cross-polarized reflection component. There are two alternatives to this standard approach. A simpler one is the use of empirical reflection damping factors along with the assumption of an isotropic antenna. A more rigorous formulation accounts for the near-field coupling between an antenna and its supporting structure.

The applicability of each type of simulator depends on the scenario. For example, a geometrical simulation may be adequate when the propagation delay represents the dominating interferometric phase component, as is typically the case in altimetry applications. A metal surface simulation is often adequate for positioning of satellites, airplanes, ships, cars, etc. On the other hand, a more complete polarimetric model becomes mandatory in interpreting the retrieval of material composition properties, such as soil moisture. A polarimetric simulator is also more realistic for the design of antennas for positioning applications, preventing an otherwise overly optimistic performance assessment under the assumption of polarization reversal (Chen et al. 2012a, b).

Sometimes one is not interested in the deterministic simulation for a specific scenario, but in the central tendency and statistical dispersion of an ensemble over varying conditions; the domain of evaluation can be any of, e.g., reflection phase, surface height, satellite direction, receiver position, etc. This integration can be derived analytically for simplified cases, generated synthetically

through Monte Carlo sampling, or measured experimentally through special data collection equipment. In their turn, such statistical distributions can be fit to parametric models for convenient reuse in later simulations.

Whereas simulators employed for positioning purposes normally assume an upright antenna, simulators for GPS-MR are typically specialized for tipped or upside-down antennas. This latter special case makes it safer to neglect complementary polarizations, and even the detailed antenna pattern under certain symmetry conditions. On the other hand, many reflectometry experiments necessitate more elaborate surface composition simulations, accounting for layering, as well as tropospheric refraction.

General design and usage

The software was designed following the principles described in Kernighan and Plauger (1982). Matlab was chosen for its outstanding plotting capabilities, adequate programming language constructs, and widespread adoption in the science and engineering fields in North America. Support for Octave was later added, as a free/libre/open-source alternative.

The installation is accomplished by simply updating the search path to ensure the routines can be found:

```
addpath(genpath(lib_dir))
```

where the library directory must be set as appropriate for the location where the simulator has been unpacked on your computer, e.g., `lib_dir = 'c:\work\m\'` for a Windows PC or `lib_dir = '~/m/'` for a computer with a UNIX-like operating system; other than that, the rest of the usage is platform-independent.

The default forward simulation (settings described below) can be run immediately by issuing the command `snr_fwd()`. It displays graphically the final multipath observables along with a textual display of the intermediate results (e.g., antenna and surface responses) on the command prompt. The graphical display can be suppressed, and the results captured by assigning the output to a return variable, as in `result = snr_fwd()`;

The code is vectorized so that multiple satellite directions, as observed from the same receiving station, are processed in batch mode rather than sequentially; this permits automatic parallel execution in computers with multiple processors or cores. Among the results, there are, e.g., `delay_interf` for the interferometric delay, `sat.elev` for the satellite elevation angle, etc. For consistency, unless otherwise specified, angles are always expressed in degrees and lengths/ranges/heights/delays in meters. Subfields provide further details, such as the following ones contained in the variable `reflected`:

```
phasor_antenna_rhcp
phasor_antenna_lhcp
phasor_fresnelcoeff_same
phasor_fresnelcoeff_cross
phasor_delay
phasor_roughness
phasor_divergence
phasor_nongeom
phasor_rhcp
phasor_lhcp
```

These are generally polarization- and direction-dependent complex-valued arrays describing the antenna radiation pattern, the surface Fresnel reflection coefficients, the surface roughness effect, etc. at each viewing direction; for example,

```
get_power(result.reflected.phasor_
fresnelcoeff_cross))
get_phase(result.reflected.phasor_
fresnelcoeff_same))
decibel_phasor
(result.direct.phasor_antenna_rhcp)
```

give, respectively, the cross-polarization power reflectivity, the same-polarization reflection phase, and the antenna RHCP gain at the satellite line of sight (in decibels).

The simulator can be customized without modifying its source code by changing the default settings, then employing these to set up the model, and finally running the forward simulation:

```
sett = snr_settings();
setup = snr_setup(sett);
result = snr_fwd(setup);
```

Routines `snr_settings()` and `snr_setup()` output matching data structures, each containing fields (namely, `ant`, `opt`, `ref`, `sat`, and `sfc`) about, respectively, the receiving antenna, general options, reference system, satellite direction, and reflecting surface. The `setup` variable is produced automatically based on the `sett` one.

Here are some examples of this pairing. The antenna/radome model is specified in `sett.ant.model` and `sett.ant.radome` (in terms of IGS `rcvr_ant.tab` codes, e.g., `TRM29659.00` and `NONE`), while the respective gain pattern is provided in `setup.ant.gain`. The electromagnetic carrier is specified in field `sett.opt.freq_name` (in terms of GPS bands, e.g., `L2`), whereas the respective frequency and wavelength values (in hertz and meters, respectively) are provided in `setup.opt.frequency` and `setup.opt.wavelength`. The height of the antenna above the surface is specified in `sett.ref.height_ant` (a scalar in meters), while

the resulting antenna phase center and antenna reference point—both three-dimensional position vectors—can be found in `setup.ref.pos_apc` and `setup.ref.pos_arp`. The satellite elevation angle limits (minimum and maximum values) are found in `sett.sat.elev_lim`, while the resulting domain of individual elevation angle values is given in `setup.sat.elev`. Lastly, the surface properties can be specified as in, e.g., `sett.sfc.material` (normally simply a name such as water, copper, etc.), which translates into `setup.sfc.permittivity` (a complex scalar).

More than one hundred such settings are available for customization, although their default values (or empty input) are often appropriate. Routine `snr_demo.m` provides a 20-page tutorial, in which the program logic is explained in plain language with snippets of source code interspersed. The principal functions—`snr_settings`, `snr_setup`, and `snr_fwd`—have documentation available via the `help` command, providing a list of input and output arguments as well as a list of accepted values (e.g., valid frequency designations).

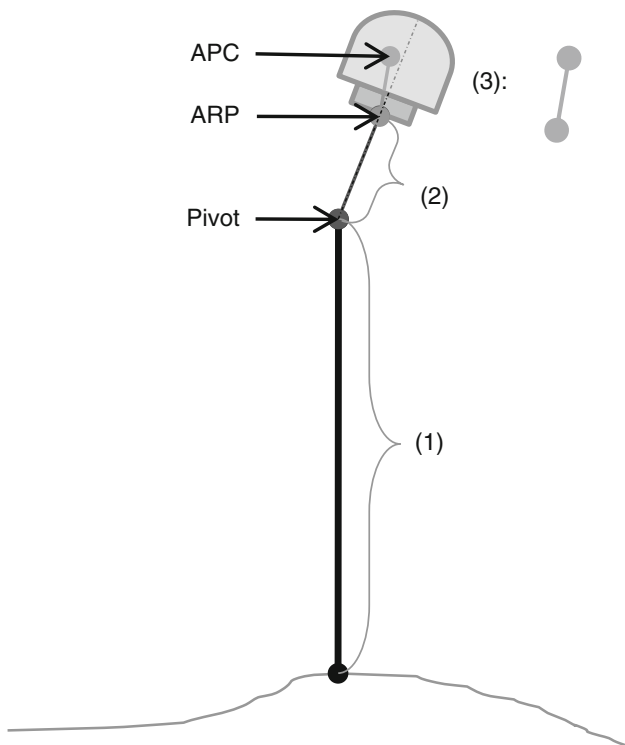


Fig. 1 The reflector height `sett.ref.height_ant`, (1) in the diagram, refers to a pivot point, the topmost position on the antenna mount that remains unchanged to rotations. There is a lever arm between the pivot and the antenna itself; its length, `sett.ref.dist_arp_pivot` (2) is rotated along with the ARP-APC vector offset (3) as per antenna orientation angles (slope, aspect, axial)

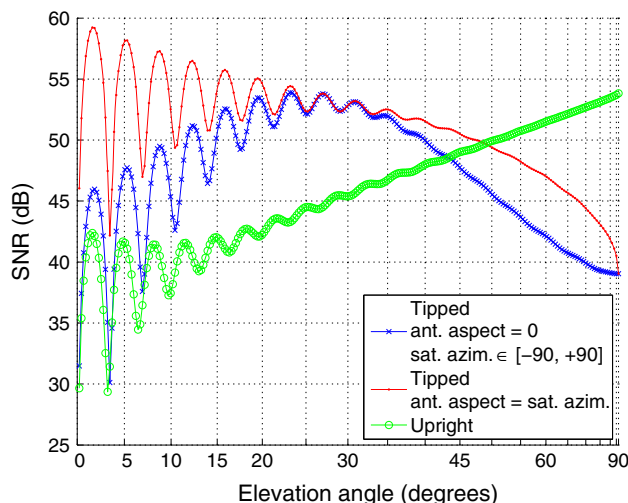


Fig. 2 Results for different antenna orientations and satellite alignment (coinciding with the antenna boresight or varying $\pm 90^\circ$ in azimuth)

Examples

Now, we illustrate three examples in more detail. All generating scripts are made available, so that the reader may reproduce results in the present simulation paper as well as in the formulation paper (Nievinski and Larson 2014a).

Surface materials

Routine `get_permittivity()` is utilized internally by `snr_setup()`; calling it directly with no input will output a list of known materials, some of which allows variable dimensional properties. For example, the variation in real and imaginary permittivity with respect to soil volumetric moisture can be obtained as follows:

```
moist_min = 0.25;
moist_max = 0.75;
moist = linspace(moist_min,
moist_max)';
material = struct('name','soil',
'moisture',moist);
perm = get_permittivity(material);
```

Antenna orientation

Whereas for positioning applications, the antenna is installed upright (i.e., with boresight facing zenith), for reflectometry often it is intentionally tipped (boresight facing the horizon); see Fig. 1 for the definition of rotation-invariant points. The antenna orientation can be specified with `sett.ant.slope`, whose value can be textual

(upright, tipped, upside-down) or numerical (respectively, 0° , 90° , 180° or any other real number). When the slope angle is nonzero, the azimuth faced by the antenna boresight can be specified in `sett.ant.aspect` (north, south, etc., or a number, 0, 180, etc.). These scalar value antenna angles can be combined with the arrays of satellite angles, to simulate a satellite crossing boresight as it rises or sets (see Fig. 2):

```
sett0 = snr_settings();
sett0.sat.elev_lim = [0 90];
sett1 = sett0;
sett1.ant.slope = 'upright';
sett2 = sett1;
sett2.ant.slope = 'tipped';
sett3 = sett2; sett3.sat.azim_lim = [-90 90];
```

Finally, `sett.ant.axial` specifies one last rotation, around the antenna axis; usually it has a less dramatic effect, because typical GPS antennas are nearly omnidirectional (axially uniform) albeit close to hemispherical (large front-to-back ratio).

Antenna gain pattern

The antenna gain pattern is normally made available as a principal plane cut (PPC), vertically across the antenna axis. This offers some information about the axial asymmetry in the antenna horizontal plane, e.g., north–south in

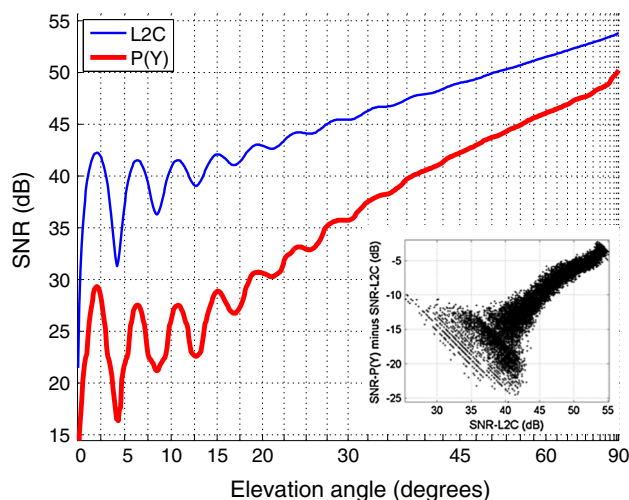


Fig. 3 SNR simulations for the same carrier frequency (L2) and receiving antenna (TRM29659.00) but different code modulations. *Inset* measured discrepancy between SNR of L2-P(Y) and of L2C, versus SNR of L2C; based on observations collected simultaneously for both codes at 10-s intervals during a full day (24 Mar 2009) at a fixed station (receiver Trimble NetRS, station P041 of the Plate Boundary Observatory, <http://pbo.unavco.org>) for all block IIR-M satellites active at the time (PRNs 7, 12, 15, 17, 29, and 31)

an upright configuration. Given irregularly spaced gain values, we fit a set of spherical harmonics (only zonal and first-order tesseral harmonics, as sectorial ones are ill-determined from a single PPC). The resulting coefficients can then be evaluated to tabulate the gain over a regularly spaced grid for subsequent faster interpolation. This pre-processing can optionally be saved to disk for later reuse. We sought to provide patterns for a number of antenna models used in GPS networks, which allows comparing their suitability for positioning and reflectometry applications. PPCs for new antennas can be incorporated as files with names such as LEIAR25__NONE__L1__LHCP__GAIN.DAT; one file for each combination of antenna model (LEIAR25, TRM41249.00, etc.), radome (NONE, SCIT), carrier frequency designation (L1, L2), polarization (RHCP, LHCP), and radiation component (gain, phase).

Code losses

The P(Y) code, in both L1 and L2 frequencies, requires (semi-)codeless tracking of the encrypted Y code when employing civilian receivers. Woo (2000) reports systematic losses, inversely proportional to SNR. These affect primarily the SNR trend but also its oscillating fringes to some extent. We have developed an empirical calibration curve based on simultaneously measured L2-P(Y) and L2C SNR (see Fig. 3); such calibrations are receiver-dependent.

The C/A is a shorter code, thus it is susceptible to cross-correlation errors, e.g., a high-power, high-elevation angle satellite creating spurious correlations when tracking a low-power rising or setting satellite. The issue seems to be exacerbated by small Doppler differences between satellites, see Lestarquit and Nouvel (2012) and the references therein. Compared to P(Y), the C/A tracking losses have a more random and less predictable behavior. Although the times of occurrence might be determined by the orbits of the GPS satellites simultaneously in view, the magnitude of the losses is less certain, e.g., certain specific PRNs are known to be more vulnerable than others. C/A losses are not currently contemplated in the simulator.

Extensions

The theoretical forward model and its software implementation in Matlab/Octave could be extended in a number of ways. As a practical matter, users would benefit from gain patterns for additional antennas as well as P(Y) SNR loss calibrations for additional receivers. Technical aspects would entail the support for additional carrier frequencies (e.g., L5) and modulations (e.g., BOC), for GPS and other GNSS as well; and different formulations for nonidealized SNR estimators (Falletti et al. 2011). Polarimetric phase

patterns are currently not made available by the antenna manufacturing companies; their future inclusion should contemplate the effect of antenna orientations: although circular polarization magnitude components are invariant under rotations, phases are not.

Some physical effects that are currently neglected deserve more consideration. These include the interferometric Doppler accumulated in dynamic scenarios such as in tidal waters (Larson et al. 2013), media layering with rough interfaces (not just rough top; Pinel et al. 2010; Tabatabaenejad et al. 2013), coherent volumetric scattering (Cloude 2009), tropospheric refraction (both in angle of arrival and in the ranging delay), and nonhorizontal surface geometry—tilted (though still planar) surfaces as well as large-scale undulations (with potentially multiple simultaneous reflections).

It is hoped that this simulator may foster the cross-fertilization across the positioning and reflectometry fields, such that developments in multipath mitigation may be leveraged for multipath exploitation, and vice versa.

Acknowledgments This research was supported by NSF (EAR 0948957, AGS 0935725). Mr. Nievinski has been supported by a Capes/Fulbright Graduate Student Fellowship (1834/07-0) and a NASA Earth System Science Research Fellowship (NNX11AL50H).

References

- Aloi D, van Graas F (1999) Analysis of the effects of Earth-surface based multipath reflections on GPS code-phase measurements. In: Proc ION AM. Institute of Navigation, Cambridge, MA, pp 609–61
- Anderson KD (2000) Determination of water level and tides using interferometric observations of GPS signals. *J Atmos Ocean Technol* 17:1118–1127. doi:10.1175/1520-0426(2000)017<1118:DOWLAT>2.0.CO;2
- Auber J-C, Bibaut A, Rigal J-M (1994) Characterization of Multipath on Land and Sea at GPS Frequencies. In: Proc ION GPS. Institute of Navigation, Salt Lake City, UT, USA, pp 1155–1171
- Bétaillé D (2003) A Testing Methodology for GPS Phase Multipath Mitigation Techniques. In: Proc ION GPS/GNSS. Institute of Navigation, Portland, OR, pp 2151–2162
- Beyerle G, Hocke K (2001) Observation and simulation of direct and reflected GPS signals in radio occultation experiments. *Geophys Res Lett* 28:1895–1898. doi:10.1029/2000GL012530
- Bilich A, Larson KM, Axelrad P (2008) Modeling GPS phase multipath with SNR: case study from the Salar de Uyuni. *Boliva. J Geophys Res* 113:B04401. doi:10.1029/2007JB005194
- Boccia L, Amendola G, Gao S, Chen C-C (2013) Quantitative evaluation of multipath rejection capabilities of GNSS antennas. *GPS Solut*. doi:10.1007/s10291-013-0321-0
- Boniface K, Aparicio JM, Cardellach E (2011) Meteorological information in GPS-RO reflected signals. *Atmos Meas Tech Discuss* 4:1199–1231. doi:10.5194/amtd-4-1199-2011
- Braasch MS (1996) Multipath effects. In: Parkinson BW, Spilker JJ, Axelrad P, Enge P (eds) *Glob. Position. Syst. Theory Appl.* AIAA, pp 547–566
- Brenner B, Reuter R, Schipper B (1998) GPS landing system multipath evaluation techniques and results. In: Proc ION GPS. Institute of Navigation, Nashville, TN, pp 999–1008
- Brodin G, Daly P (1997) GNSS code and carrier tracking in the presence of multipath. *Int J Satell Commun* 15:25–34. doi:10.1002/(SICI)1099-1247(199701)15:1<25:AID-SAT565>3.0.CO;2-F
- Byun SH, Hajj GA, Young LE (2002) Development and application of GPS signal multipath simulator. *Radio Sci* 37:1098. doi:10.1029/2001RS002549
- Cardellach E, Fabra F, Rius A, Pettinato S, D’Addio S (2012) Characterization of dry-snow sub-structure using GNSS reflected signals. *Remote Sens Environ* 124:122–134. doi:10.1016/j.rse.2012.05.012
- Chen A, Chabory A, Escher A, Macabiau C (2009) Development of a GPS deterministic multipath simulator for an efficient computation of the positioning errors. In: Proc ION GNSS. Institute of Navigation, Savannah, GA, pp 2378–2390
- Chen A, Chabory A, Escher A, Macabiau C (2010) Hybrid deterministic-statistical GPS multipath simulator for airport navigation. In: Bonefačić D, Bosiljevac M (eds) *IECom—20th Int. Conf. Appl. Electromagn. Commun*, Dubrovnik, Croatia, pp 3–6
- Chen C-C, Gao S, Maqsood M (2012a) Antennas for Global Navigation Satellite System Receivers. In: Imbriale WA, Gao S, Boccia L (eds) *Space Antenna Handbook*. Wiley, pp 548–595
- Chen X, Parini CG, Collins B, Yao Y, Ur Rehman M (2012b) Antennas for global navigation satellite systems. Wiley, p 232
- Chew CC, Small EE, Larson KM, Zavorotny VU (2013) Effects of Near-Surface Soil Moisture on GPS SNR Data: Development of a Retrieval Algorithm for Soil Moisture. *IEEE Trans Geosci Remote Sens* 1–7. doi:10.1109/TGRS.2013.2242332
- Cloude S (2009) *Polarisation: applications in remote sensing*. Oxford
- Cox DT, Shallberg KW, Manz A (2000) Definition and analysis of WAAS receiver multipath error envelopes. *Navigation* 46:271–282
- Eissfeller B, Winkel JO (1996) GPS Dynamic Multipath Analysis in Urban Areas. In: Proc ION GPS, Institute of Navigation, Kansas City, MO, pp 719–727
- Elósegui P, Davis JL, Jaldehag RTK, Johansson JM, Niell AE, Shapiro II (1995) Geodesy using the global positioning system: the effects of signal scattering on estimates of site position. *J Geophys Res* 100:9921. doi:10.1029/95JB00868
- Ercek R, de Doncker P, Grenez F (2005) Study of pseudo-range error due to non-line-of-sight-multipath in urban canyons. In: Proc ION GNSS. Institute of Navigation, Long Beach, CA, pp 1083–1094
- Evans J, Capon J, Shnidman D (1989) Multipath modeling for simulating the performance of the microwave landing system. *Linc Lab J* 2:459–474
- Falletti E, Pini M, Lo L Presti (2011) Low complexity carrier-to-noise ratio estimators for GNSS digital receivers. *IEEE Trans Aerosp Electron Syst* 47:420–437. doi:10.1109/TAES.2011.5705684
- Fan K, Ding XL (2006) Estimation of GPS carrier phase multipath signals based on site environment. *J Glob Pos Syst* 5:22–28. doi:10.5081/jgps.5.1.22
- Franchois A, Roelens L (2005) Determination of GPS positioning errors due to multi-path in civil aviation. In: Proc. 2nd Int. Conf. Recent Adv. Space Technol. RAST 2005. pp 400–403
- Georgiadou Y, Kleusberg A (1988) On carrier signal multipath effects in relative GPS positioning. *Manuscripta Geod* 12:172–179
- Geren W, Murphy T, Pankaskie T (2008) Analysis of airborne GPS multipath effects using high-fidelity EM models. *IEEE Trans Aerosp Electron Syst* 44:711–723. doi:10.1109/TAES.2008.4560216
- Gomez S, Panneton R, Saunders P, Hwu S, Lu B (1995) GPS multipath modeling and verification using geometrical theory of diffraction. In: Proc ION GPS. Institute of Navigation, Palm Springs, CA, pp 195–204

- Hannah BM, Walker RA, Kubik K (1998) Towards a complete virtual multipath analysis tool. In: Proc ION GPS. Institute of Navigation, Nashville, TN, pp 1055–1063
- Irsigler M, Avila-Rodriguez JA, Hein GW (2005) Criteria for GNSS multipath performance assessment. In: Proc ION GNSS. Institute of Navigation, Long Beach, CA, pp 2166–2177
- Italiano A, Principe F (2010) Multipath and interference modelling in complex GNSS scenarios. In: Proc. 4th Eur. Conf. Antennas Propag. EuCAP. pp 1–5
- Jacobson MD (2008) Dielectric-covered ground reflectors in GPS multipath reception: theory and measurement. *IEEE Geosci Remote Sens Lett* 5:396–399. doi:[10.1109/LGRS.2008.917130](https://doi.org/10.1109/LGRS.2008.917130)
- Kalyanaraman SK, Braasch MS, Kelly JM (2006) Code tracking architecture influence on GPS carrier multipath. *IEEE Trans Aerosp Electron Syst* 42:548–561. doi:[10.1109/TAES.2006.1642571](https://doi.org/10.1109/TAES.2006.1642571)
- Kavak A, Vogel WJ, Xu G (1998) Using GPS to measure ground complex permittivity. *Electron Lett* 34:254–255. doi:[10.1049/el:19980180](https://doi.org/10.1049/el:19980180)
- Kelly J, Cohenour J, DiBenedetto MF, Lamb D (2004) An advanced multipath model for DGPS reference site analysis. In: Proc ION AM. Institute of Navigation, Dayton, OH, pp 315–327
- Kernighan BW, Plauger PJ (1982) The elements of programming style, (2nd edn). McGraw-Hill, p 168
- King MA, Watson CS (2010) Long GPS coordinate time series: multipath and geometry effects. *J Geophys Res.* doi:[10.1029/2009JB006543](https://doi.org/10.1029/2009JB006543)
- Larson KM, Ray RD, Nievinski FG, Freymueller JT (2013) The accidental tide gauge: a GPS reflection case study from kachemak bay Alaska. *IEEE Geosci Remote Sens Lett* 10(5):1200–1204. doi:[10.1109/LGRS.2012.2236075](https://doi.org/10.1109/LGRS.2012.2236075)
- Lau L, Cross P (2007) Development and testing of a new ray-tracing approach to GNSS carrier-phase multipath modelling. *J Geod* 81:713–732. doi:[10.1007/s00190-007-0139-z](https://doi.org/10.1007/s00190-007-0139-z)
- Lestarquit L, Nouvel O (2012) Determining and measuring the true impact of C/A code cross-correlation on tracking: application to SBAS georanging. In: Proc IEEE/ION PLANS. IEEE, pp 1134–1140
- Lippincott W, Milligan T, Igli D (1996) Method for calculating multipath environment and impact on GPS receiver solution accuracy. In: Proc ION NTM. Institute of Navigation, Santa Monica, CA, pp 707–722
- Löfgren JS, Haas R, Scherneck H-G, Bos MS (2011) Three months of local sea level derived from reflected GNSS signals. *Radio Sci* 46:1–12. doi:[10.1029/2011RS004693](https://doi.org/10.1029/2011RS004693)
- Lopez AR (2008) LAAS/GBAS ground reference antenna with enhanced mitigation of ground multipath. In: Proc ION NTM. Institute of Navigation, San Diego, CA, pp 389–393
- Luo X, Mayer M, Heck B (2008) Improving the stochastic model of GNSS observations by means of SNR-based weighting. *Obs. Our Chang. Earth.* Springer, pp 725–734
- Macabiau C, Roturier B, Chatre E, Renard A (1999) Airport multipath simulation for siting DGPS reference stations. In: Proc ION NTM. Institute of Navigation, San Diego, CA, pp 135–144
- Mironov VL, Fomin SV, Muzalevskiy KV, Sorokin AV, Mikhaylov MI (2012) The use of navigation satellites signals for determination the characteristics of the soil and forest canopy. *IEEE IGARSS.* pp 7527–7529
- Mora-Castro EJ, Carrascosa-Sanz C, Ortega G (1998) Characterisation of the multipath effects on the GPS pseudorange and carrier phase measurements. In: Proc ION GPS. Institute of Navigation, Nashville, TN, pp 1065–1074
- Nievinski FG, Larson KM (2014a) Forward modeling of GPS multipath for near-surface reflectometry and positioning applications. *GPS Solut* 18(2):309–322. doi:[10.1007/s10291-013-0331-y](https://doi.org/10.1007/s10291-013-0331-y)
- Nievinski FG, Larson KM (2014b) Inverse modeling of GPS multipath for snow depth estimation—Part I: formulation and simulations. *IEEE Trans Geosci Remote Sens.* doi:[10.1109/TGRS.2013.2297681](https://doi.org/10.1109/TGRS.2013.2297681)
- Ozeki M, Heki K (2011) GPS snow depth meter with geometry-free linear combinations of carrier phases. *J Geod* 86:209–219. doi:[10.1007/s00190-011-0511-x](https://doi.org/10.1007/s00190-011-0511-x)
- Pinel N, Bourlier C, Saillard J (2010) Degree of roughness of rough layers: extensions of the rayleigh roughness criterion and some applications. *Prog Electromagn Res B* 19:41–63. doi:[10.2528/PIERB09110907](https://doi.org/10.2528/PIERB09110907)
- Ray JK, Cannon ME (2001) Synergy between global positioning system code, carrier, and signal-to-noise ratio multipath errors. *J Guid Control Dyn* 24:54–63. doi:[10.2514/2.4675](https://doi.org/10.2514/2.4675)
- Rigden GJ, Elliott JR (2006) 3dM: a GPS receiver antenna site evaluation tool. In: Proc ION NTM. Institute of Navigation, Monterey, CA, pp 554–563
- Rodgers CE (1992) Multipath simulation software developed for the design of a low multipath DGPS antenna for the US coast guard. In: Proc ION GPS. Institute of Navigation, Albuquerque, NM, pp 43–50
- Rodriguez-Alvarez N, Camps A, Vall-Ilossera M, Bosch-Lluis X, Moneris A, Ramos-Perez I, Valencia E, Marchan-Hernandez JF, Martinez-Fernandez J, Baroncini-Turricchia G, Perez-Gutierrez C, Sanchez N (2011) Land geophysical parameters retrieval using the interference pattern GNSS-R technique. *IEEE Trans Geosci Remote Sens* 49:71–84. doi:[10.1109/TGRS.2010.2049023](https://doi.org/10.1109/TGRS.2010.2049023)
- Schubert FM, Prieto-Cerdeira R, Robertson P, Fleury BH (2009) SNACS: the satellite navigation radio channel signal simulator. In: Proc ION GNSS. Institute of Navigation, Savannah, GA, pp 1982–1988
- Smyrnaios M, Schn S, Liso M (2013) Multipath propagation, characterization and modeling in GNSS. In: S. Jin (Ed.), *Geodetic sciences: observations, modeling and applications*, doi:[10.5772/54567](https://doi.org/10.5772/54567), p. 99–124.
- Steingass A, Lehner A, Pérez-Fontán F, Kubista E, Arbesser-Rastburg B (2008) Characterization of the aeronautical satellite navigation channel through high-resolution measurement and physical optics simulation. *Int J Satell Commun Netw* 26:1–30. doi:[10.1002/sat.891](https://doi.org/10.1002/sat.891)
- Tabatabaenejad A, Duan X, Moghaddam M (2013) Coherent scattering of electromagnetic waves from two-layer rough surfaces within the Kirchhoff regime. *IEEE Trans Geosci Remote Sens* 51:3943–3953. doi:[10.1109/TGRS.2012.2229391](https://doi.org/10.1109/TGRS.2012.2229391)
- Treuhaft RN, Lowe ST, Zuffada C, Chao Y (2001) 2-cm GPS altimetry over Crater Lake. *Geophys Res Lett* 28:4343. doi:[10.1029/2001GL013815](https://doi.org/10.1029/2001GL013815)
- van Nee RDJ (1992) Multipath effects on GPS code phase measurements. *Navigation* 39:177–190
- Weiss J, Axelrad P, Anderson S (2007) A GNSS code multipath model for semi-urban, aircraft, and ship environments. *Navigation* 54:293–307
- Woo KT (2000) Optimum semi codeless carrier-phase tracking of L2. *Navigation* 47:82–99
- Zavorotny VU, Larson KM, Braun JJ, Small EE, Gutmann ED, Bilich AL (2010) A physical model for GPS multipath caused by land reflections: toward bare soil moisture retrievals. *IEEE J Sel Top Appl Earth Obs Remote Sens* 3:100–110. doi:[10.1109/JSTARS.2009.2033608](https://doi.org/10.1109/JSTARS.2009.2033608)
- Zhu Z, van Graas F (2009) Earth-surface multipath detection and error modeling for aircraft GPS receivers. *Navigation* 56:45–56



Felipe G. Nievinski received the B.E. degree in geomatics from Universidade Federal do Rio Grande do Sul (UFRGS), Porto Alegre, Brazil, in 2005; the M.Sc.E. degree in geodesy from the University of New Brunswick, Fredericton, NB, Canada, in 2009; and the Ph.D. degree in aerospace engineering sciences from the University of Colorado Boulder, Boulder, CO, USA, in 2013. He is a Postdoctoral Researcher with Universidade Estadual Paulista “Júlio

de Mesquita Filho” (UNESP), Presidente Prudente, Brazil, where he works in the field of GPS multipath reflectometry.



Kristine M. Larson received the B.A. degree in engineering sciences from Harvard University, Cambridge, MA, USA, in 1985 and the Ph.D. degree in geophysics from the Scripps Institution of Oceanography, University of California at San Diego, La Jolla, CA, USA, in 1990. She is a professor of aerospace engineering sciences with the University of Colorado Boulder, Boulder, CO, USA. Her current research focuses on GPS reflections.